Solid Freeform Fabrication 2019: Proceedings of the 30th Annual International
Solid Freeform Fabrication Symposium – An Additive Manufacturing Conference
Reviewed Paper

A Multi-scale Computational Model to predict the performance of Cell Seeded Scaffolds with Triply Periodic Minimal Surface Geometries

E.F. Lehder*, I.A. Ashcroft*, R.D. Wildman*, I. Maskery*, L.R. Cantu*

*Centre for Additive Manufacturing, Faculty of Engineering, University of Nottingham, Nottingham NG8 1BB, UK

Abstract

Bone scaffolds are required to replace the painful and dangerous process of bone grafting, currently the gold standard for treating open bone fractures. Tissue engineering scaffolds work best when there is a high amount of surface area for biological cells to attach. Triply Periodic Minimal Surface (TPMS) geometries offer high ratios of surface area per volume. However, it is not yet clear which TPMS cell type would yield the fastest bone growth rate. In this study, we used a three-dimensional multi-scale model to predict the performance of scaffolds with four TPMS unit cell types (Primitive, Gyroid, Diamond and Lidinoid). At the micro-scale, the model simulates curvature-dependent tissue growth, while at the macro-scale the model uses FEA to ensure the construct stiffness is acceptable. The Lidinoid unit cell type was found to yield the most bone growth after 40 days while also ensuring an acceptable scaffold stiffness.

KEYWORDS
Bone scaffolds, Computational modelling, Minimal surfaces, Tissue regeneration, Level set method, Multi-scale

1 Introduction

Currently the standard procedure to aid in the healing of bone defects or fractures is the use of bone allograft (bone graft from another patient) or autograft (bone graft from the patient with the bone defect/fracture). The latter leads to the best results because the graft is highly compatible with the surrounding bone given that it comes from the patient her/himself [1]. However, there are several drawbacks of these processes: limited material availability, longer operation time as bone needs to be both removed and implanted, increased blood loss and pain, as well as other potential complications at the donor site [2]. Alternatives to natural bone grafts are engineered synthetic bone grafts. Synthetic graft materials such as Calcium phosphate (CaP), tricalcium phosphate (TCP) and hydroxyapatite possess mechanical properties like those of the organic part of bone. However, for cells to migrate, attach, proliferate and differentiate, an adequate porous structure is necessary [3]. Traditional manufacturing techniques cannot accurately control the porous architecture of a scaffold and are limited to one single material. Additive manufacturing on the other hand, allows for accurate control of the porous geometry to be used and with certain techniques it is also possible to construct multi-material scaffolds [3].

Minimal surfaces are surfaces that locally minimise their surface energy, which is the same as saying they have a mean curvature of zero [4][5]. These geometries are very attractive for tissue engineering applications, not only because they resemble the porous geometry of trabecular bone, which was also observed to have a mean curvature close to zero [6]; but because they maximize the surface area to volume ratio of a scaffold, thus allowing for higher cell attachment as compared to other geometries [5]. Various studies have looked at the effect of different Triply Periodic Minimal Surface (TPMS) parameters on a scaffold's performance [7][8][7] but they have not done this combining time-dependency as well as multiple scales. Time dependency is important because at different stages of the cell development process the curvature profile of a scaffold will change as well as its porosity and pore size. Therefore, an analysis that only considers the initial scaffold before tissue growth is not thorough enough. Considering multiple scales is important because it should be ensured that the scaffold has a sufficient mechanical integrity to bear loads while at the same time allowing for optimal cell development conditions.

A key challenge in tissue engineering is finding the scaffold input parameters that provide the best performance parameters for a given case. In order to understand how all the above parameters affect the performance of scaffolds, intuitively one would think of testing different options *in vivo* or *in vitro* and comparing their outcome. However, there are too many input parameters and the number of possible combinations is thus much greater. This would make thorough *in vitro* or *in vivo* analyses extremely expensive and time consuming. Computational modelling is a potential solution for both of these problems [8]. If one could computationally predict the effect that the input scaffold parameters have on the performance parameters (with enough accuracy), then there would be no need for extensive *in vivo* or *in vitro* testing. Instead, *in vitro* and *in vivo* studies would serve only as a way of validating the computational models.

The work done until 2016 on computational modelling on how cell-scaffold interactions affect the tissue formation has been thoroughly reviewed [8]. These articles as well as articles from 2016 on have been reviewed here using the following keyword criteria: "modelling" AND ("bone regeneration scaffold" OR "tissue regeneration scaffold"). There are multiple physics fields as well as multiple scales involved in the tissue regeneration process. The main physics fields involved are solid mechanics, fluid mechanics and biochemistry. The most important scales are the tissue-scale (macro-scale), the pore-scale (micro-scale) and the cell-scale (nano-scale). The review concluded amongst other things that the inclusion of the multiple physics fields as well as length scales involved is crucial to develop an accurate model. The review article also concludes that multi-scale models are important especially because it should be ensured that the scaffold has a sufficient mechanical integrity to bear loads while at the same time allowing for optimal cell development conditions. The figures below show the physics fields as well as length scales that the modelling studies have so far focused on.

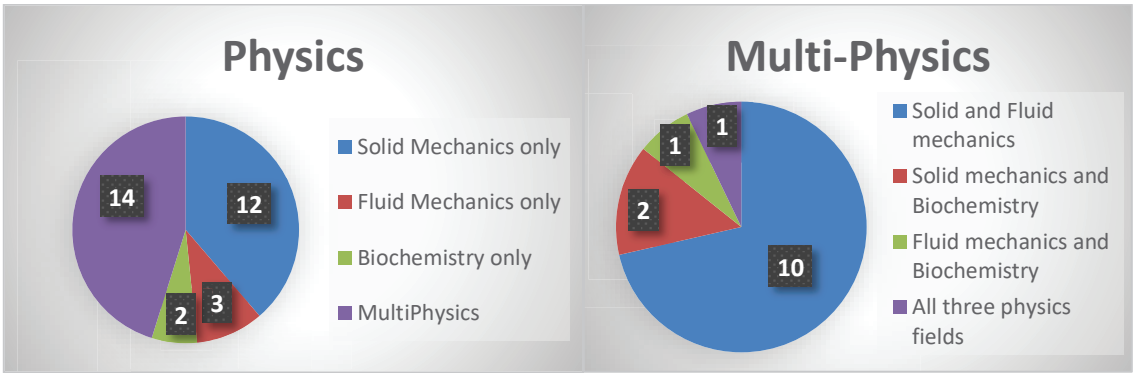

Figure 1: Pie chart showing the number of papers reviewed that focused on each of the three physics fields involved in the tissue regeneration process

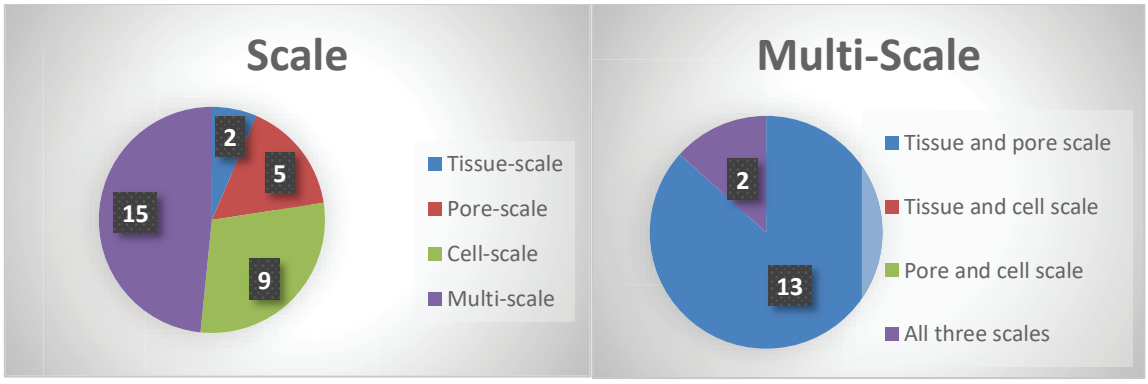

Figure 2: Pie charts showing the number of papers that focused on a given length-scale or on multiple scales.

At scales larger than the cell (what is named here the pore scale) mathematical models usually need to answer two main observations: a) the rate of bone tissue regeneration increases with increasing concave curvature and b) No regeneration is observed on planar or convex structures. The work of a particular group (The department of

Biomaterials in the Max Planck Institute of Colloids and Interfaces) [9] [10] [6] has been essential towards our understanding of the effect of geometry on tissue growth. In 2008 their pioneering work [9] proved the aforementioned observations and suggested that the dependence of tissue growth on geometrical features is due to mechanical forces that develop at the surface of the scaffold. Higher curvature results in higher stress concentration and thus higher levels of tissue regeneration stimulus. The fact that tissue grows on concave surfaces but not in convex ones was explained by the "presence of contractile tensile stresses produced by cells near the tissue surface" [6]. These surface stresses could prevent tissue from growing on convex surfaces. However, after a delay period tissue will begin to grow even on flat and convex regions as tissue layers from other regions approach the flat or convex regions.

The theories about how geometry affects cell growth can be helpful by using them to predict tissue regeneration performance and thus find optimal geometries. One type of model that can be used for this purpose is one where some tissue regeneration output variable is directly linked to a geometrical input parameter such as curvature. A recent example of such a model is presented in the work of Guyot et al. [11] where the relationship between surface curvature and the rate of tissue growth, derived by Rumpler et al. [10], was combined with the level set method in order to predict the tissue growth of an initial layer of cells attached to the surface of a scaffold. The mentioned study was validated and computational results agreed well with experiments. Images of the cell seeded scaffolds after 7 and 14 days served as validation but also the values of 'projected tissue area' that were measured using the Live-Dead viability method and compared to the modelling results (also after 7 and 14 days of culture).

The aim of this work was the development of a computational method for comparison and optimization of TPMS scaffold geometries in order to maximize their regenerative capacity while ensuring sufficient mechanical performance. As mentioned before there have been other works that attempted to model the performance of TPMS scaffolds but they did not include necessary factors such as time-dependency or a measure of mechanical performance.

2 Multi-scale model

2.1 Micro-scale tissue regeneration model

The micro-scale model chosen was that of Guyot et al. [11] which assumes that the tissue growth rate on a cell seeded scaffold is directly linked to the local curvature on the scaffold surface. This assumption was first validated by Rumpler et al. [10]. The model is particularly convenient because by using the level set method, it works with any geometry. The level set method is very useful for tracking a moving interface [12]. It is interesting to note that this curvature-dependent technique predicts the spreading of fire to be very similar to the growth of tissue. It appears that various processes in nature develop in a curvature-dependent manner. This can also be viewed from an energy minimising perspective, which is in fact how the theory was derived.

The level set method works by updating a distance function at every time step. If working with pixels in two dimensions, this method can be visualized by giving every pixel a value equal to its distance from a given contour, as illustrated in the figure below (the distance value is represented by the color). The contour in red represents a curve that is 0.5 pixels away (at every point) from the curve to which the distance from each pixel is being measured. At any point on this line the distance function is therefore equal to 0.5. Mathematically, if the distance function is $\boldsymbol{\varphi}$ then the advection equation below describes the tracking of the red contour in the whole domain Ω [11]. The hypothesis that this whole concept relies on is that the development of this interface is representative of the tissue growth on a cell seeded tissue regeneration scaffold.

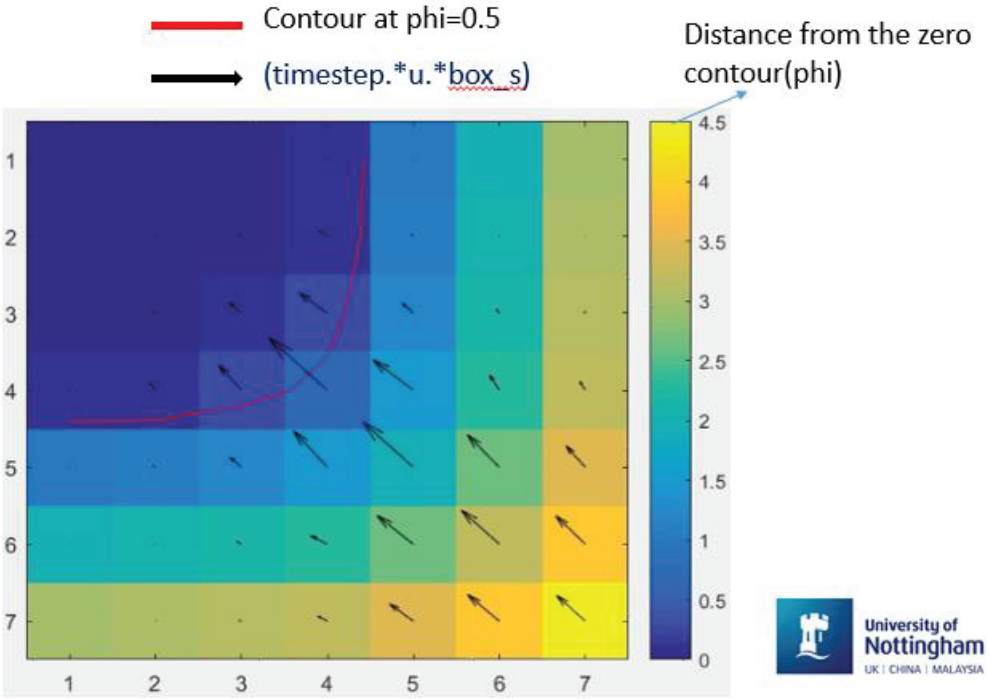

Figure 3: pixels plot showing the interface contour (red) at a given time step. This represents the interface between the growing tissue and the pore (darker blue). As shown, the pixel values represent the distance from the zero contour. The arrows represent the growth rate at any given pixel.

$$\frac{\partial \varphi}{\partial t} + u * \nabla \varphi = 0 \;\; in \;\; \Omega$$

Equation 1: Level set equation for the whole domain

$$u = \begin{cases} -kn & if \; k > 0 \\ 0 & if \; k \leq 0 \end{cases}$$

Equation 2: Interface growth velocity

$$n = \frac{\nabla \varphi}{|\nabla \varphi|}$$

Equation 3: Unit vector showing the direction of the velocity

$$k = \nabla * \mathrm{n}$$

Equation 4: Curvature definition

The interface advection velocity **u** is zero where the curvature k is equal or lower than zero, and where the curvature is higher than zero it is equal to the product of **k** and the normal unit vector **n** [11]. This definition of the advection velocity was based on the pioneering work of Rumpler et al. [10]. As can be seen, both the normal unit vector **n** and the curvature **k** are functions of the resultant gradient of the distance function. The black arrows in the figure above represent the increase in the distance from the relevant pixel to the zero contour (interface).

2.2 Macro-scale mechanical performance model

At the macro-scale it was decided that a Finite Element model would be best for predicting the scaffold stiffness which could serve as a suitable indication of the mechanical performance of the scaffold. The Finite Element Method has previously been shown to be very useful for analysing the mechanical response of tissues [13]. Recently, a study performed by I. Maskery et al. [14] used the Finite Element method to analyse the effect of cell type, orientation and volume fraction of TPMS structures on the stiffness of the scaffold in different directions. The study then went on to determine numerical constants for an equation that has been shown to determine the stiffness of a TPMS scaffold **E** given the volume fraction $\boldsymbol{\rho}$ and the loading direction **d**:

$$E^*(d) = C_1(d)\rho^{*n(d)} + E_0^*(d)$$

Equation 5: Equation to calculate the relative young's modulus of a TPMS scaffold. The C1, n and E0 terms must be determined for the given material and number of unit cells.

The process to determine these constants was repeated here given that while the constants for the Primitve, Gyroid and Diamond cell types had been determined, this had not been done for the Lidinoid cell type. The first step was to set up a MATLAB script that generates the required input file for ABAQUS to run Finite Element simulations and output the stiffness of the scaffold. For this, the script had to first create a mesh based on a given TPMS geometry (created using Flatt Pack), followed by generating an input text file for ABAQUS with the required material, loading and boundary conditions. Next, the script was set to run ABAQUS and finally read its output file that contained the stiffness calculated for that given geometry. The material was set to have a homogeneous young's modulus of 1GPa, the loading applied was a tensile load normal to the top surface of the scaffold (it was only applied to the nodes on the top surface) depicted as the [001] direction in the figure below.

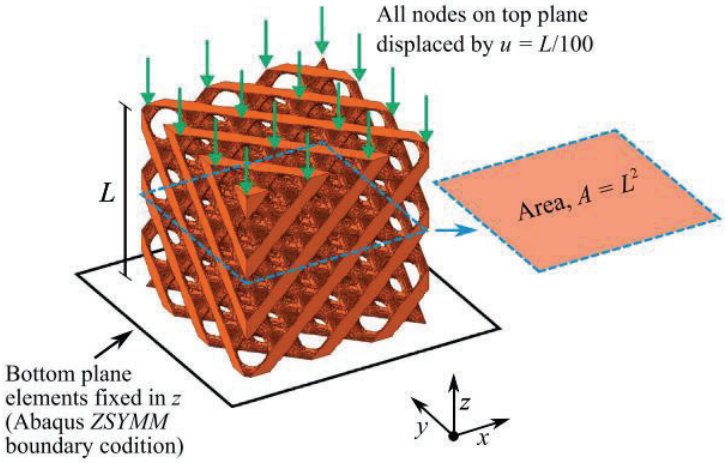

Figure 4: Geometry of a diamond cell type TPMS scaffold showing the loading as well as boundary conditions applied. Taken from the work of Maskery [14].

2.3 Multi-scale simulation scheme

The two models described above were combined into one, such that for a given value of volume fraction, the two output parameters are calculated. First, the tissue generation capacity of the scaffold is analysed on one of the pores by calculating the volume of tissue generated after a given number of days (usually 21 days to be consistent with most cell culturing studies). Then the mechanical performance is also quantified by calculating the stiffness of the scaffold at the tissue-scale (this could also be adapted to the shape of a given bone eventually) is calculated using either a Finite Element Model or a numerical model with the derived constants (a Finite Element model would be required if this were to be shape-specific, but in the current state of the study it is not). This scheme could then be used for an optimization as shown in the figure below, where the scaffold stiffness is the constraint and the tissue volume after the given simulation time (which corresponds to 21 days of cell culture) is the objective function. The design variable to be optimised would be the volume fraction of the structure. The number of unit cells as well as the size of the scaffold would then be constant.

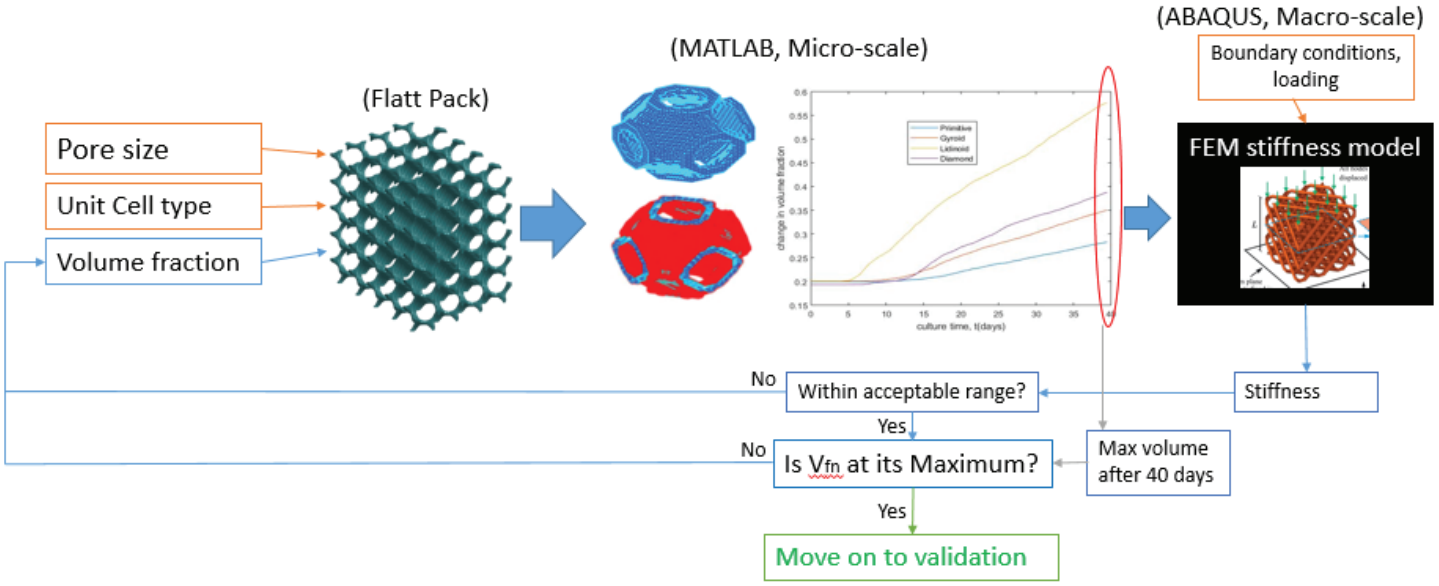

Figure 5: Schematic of the multi-scale strategy to optimize the volume fraction of the scaffold.

3. Results and Discussions

3.1 Micro-scale modelling with TPMS scaffolds

Triply Periodic Minimal Surface (TPMS) geometries of four different cell types were used to test how the model applies to three dimensional complex geometries. These were Primitive, Gyroid, Lidinoid and Diamond cell types. The volume fraction was initially 0.2 for all of them and the total cubic volume was 27 voxels cubed. Each voxel was 1µm^3. The predictive model was then ran for these four cell types and the increase in volume fraction was recorded for every iteration. The results for each cell type were then compared. The figure further below shows how the model predicts a change in the volume fraction over the cell culturing period of 40 days.

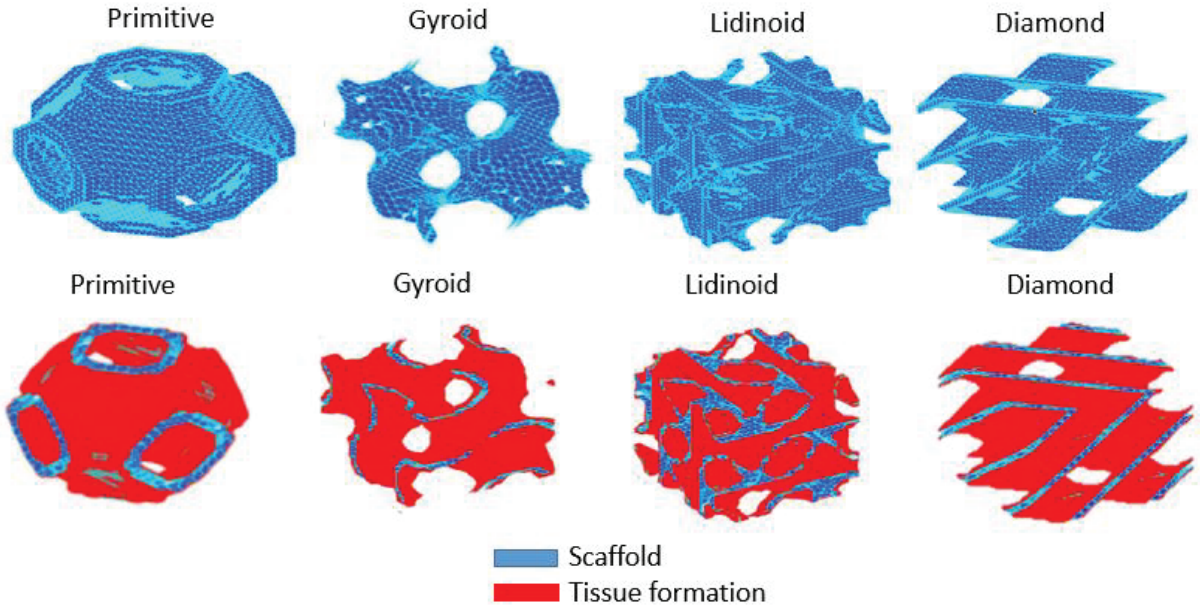

Figure 6: (Top) The different triply periodic minimal surface (TPMS) shapes used in this study. All at 0.2 volume fraction. (Bottom) The different triply periodic minimal surface (TPMS) scaffolds after tissue has been predicted to grow on them for 20 days of culture.

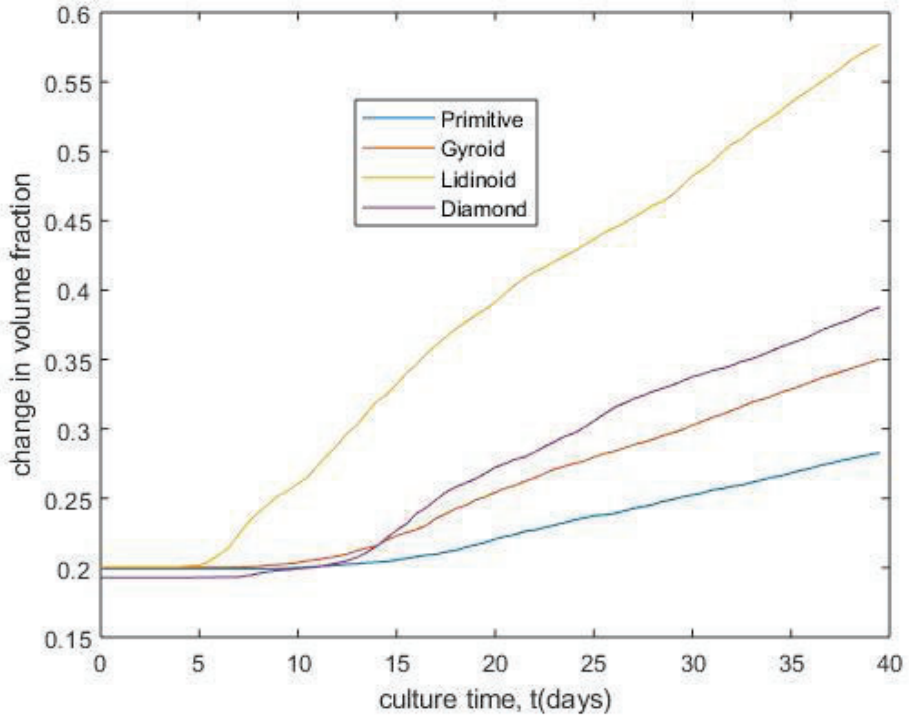

Figure 7: The change in volume fraction for each cell type after a simulation time equivalent to 40 days. As can be seen they all start roughly at the same volume fraction (20%).

As can be observed, the Lidinoid cell type appears to yield the fastest tissue growth rate according to the model, followed by the Diamond, Gyroid and Primitive cell types respectively. A further study of the effect that increasing the volume density of the scaffold has on the tissue generation was conducted and the results are presented in the figures below. This shows that the change in tissue volume fraction decreases as the initial volume fraction of the scaffold is increased. A convergence study was done by increasing the number of voxels used per dimensional length. Using this it was possible to define the minimum required number of voxels to represent the geometries.

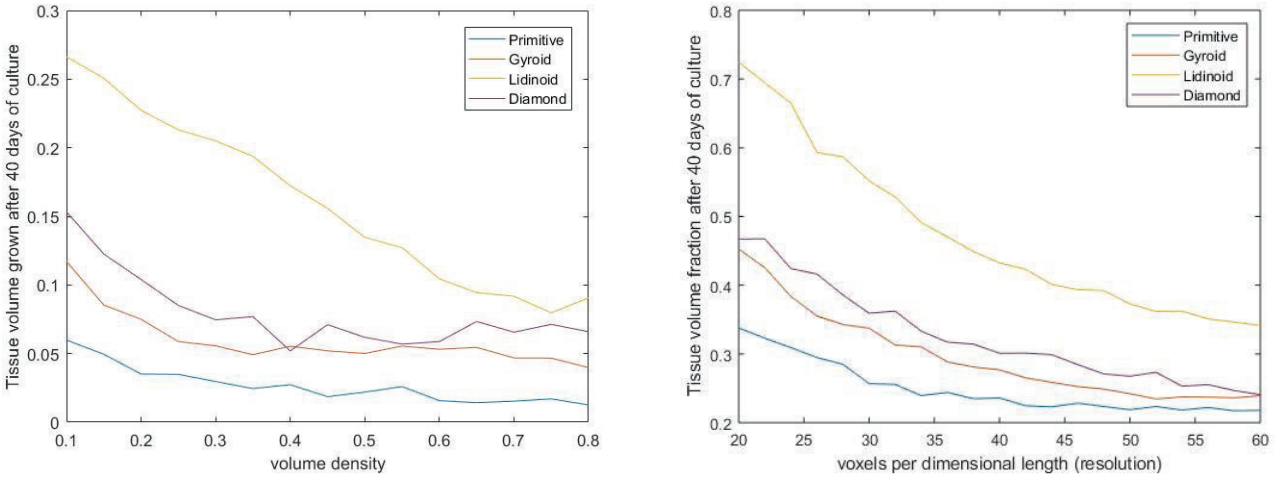

Figure 8: (Left) Change in the tissue formed on each of the TPMS cell types after 40 culture days vs the change in volume density. (Right) Same y-axis as on the left but now the x-axis represents the change in voxels per dimensional length. Volume density is represented here as a fraction of the total volume.

3.2 Macro-scale model for mechanical performance of scaffold

The determined constants are shown in the table below. As stated previously, the curve fitting process was carried out in a previous study for the Primitive, Gyroid and Diamond cell types [15] but the process was repeated here for the Lidinoid type, as it had not been done previously. The below curve shows the power fit that was done in MATLAB using the results from the Finite Element Modeling that was carried out in ABAQUS. The figure also shows the resulting constants for the power function and some measures for the goodness of the fit.

Table 1: Constants for the stiffness-volume fraction relationship

Cell type	C1	n	E0
Primitive	0.92	0.9	-0.199
Gyroid	1.06	2.4	0.006
Diamond	0.78	2.2	0.005
Lidinoid	1.41	3.5	0.008

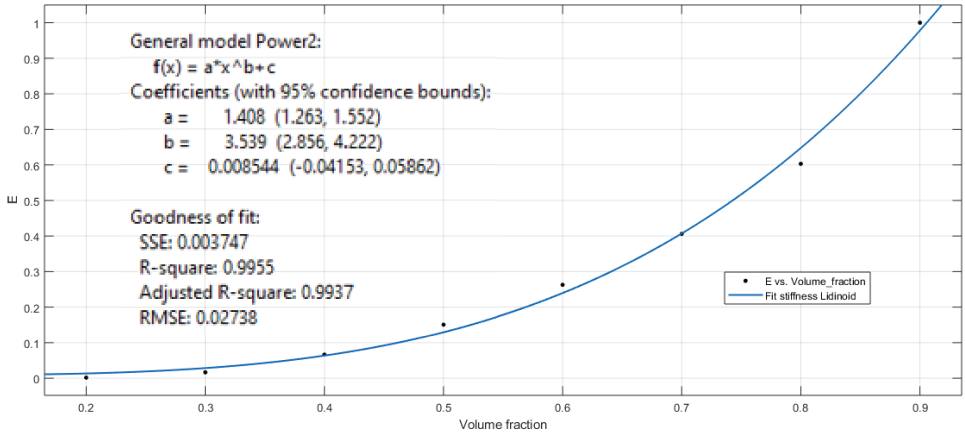

Figure 9: Fitting a power curve to Finite Element Modelling results for the stiffness (E) with varying the volume fraction.

The figure below shows how the stiffness varies with changes in the volume fraction of TPMS scaffolds with Primitive, Gyroid, Diamond and Lidinoid cell types. It can be seen that while at lower volume fractions the primitive cell type achieves the highest stiffness, at higher volume fractions the Lidinoid type yields the stiffest scaffold. It should be noted that while the derived constants are different with increasing the number of unit cells, it has been shown that after about four unit cells the change in the elastic modulus is negligible [15]. Hence why a four by four by four scaffold was used here. In future work this should take into account the geometry of the patients fracture; the model would then be patient-specific.

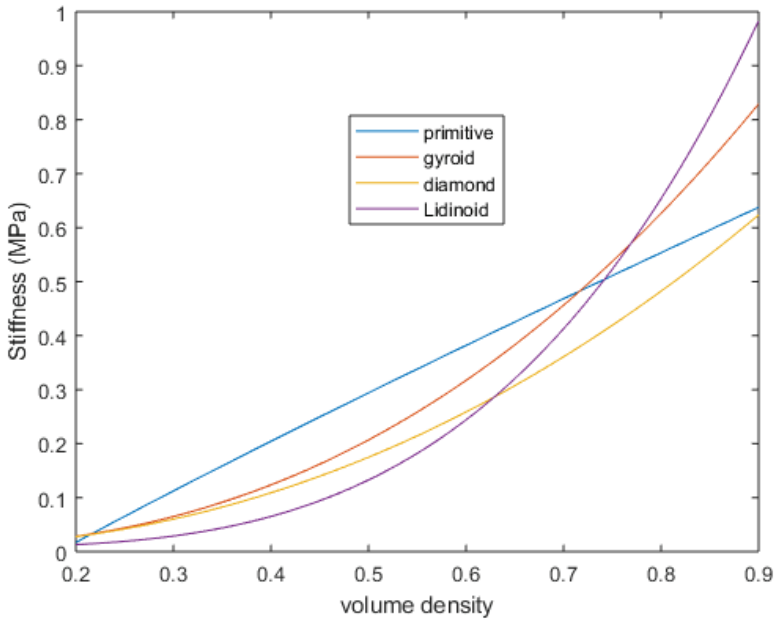

Figure 10: Change in stiffness of the scaffolds vs change in the volume fraction.

3.3 Multi-scale simulation scheme

Given the trend of the scaffold relative stiffness, a graphical optimization could be carried out here. In the figure below, if the minimum relative stiffness value is defined as 0.3, a horizontal line could be drawn perpendicular to the y-axis at that point as shown below. At the intersection between this line and the relative scaffold stiffness curve (orange) a vertical line can then be drawn as shown and finally where this line intersects the Tissue volume fraction curve (blue) is the minimum volume fraction that can be achieved. The maximum value of Tissue volume between that volume fraction and the maximum then yields the optimal volume fraction, 0.63 in this case. In a real optimization study the constraint should be selected carefully as well as the upper and lower bounds, and the optimization algorithm should be computer based rather than human eyes. A gradient-based algorithm would work well in a case like this one.

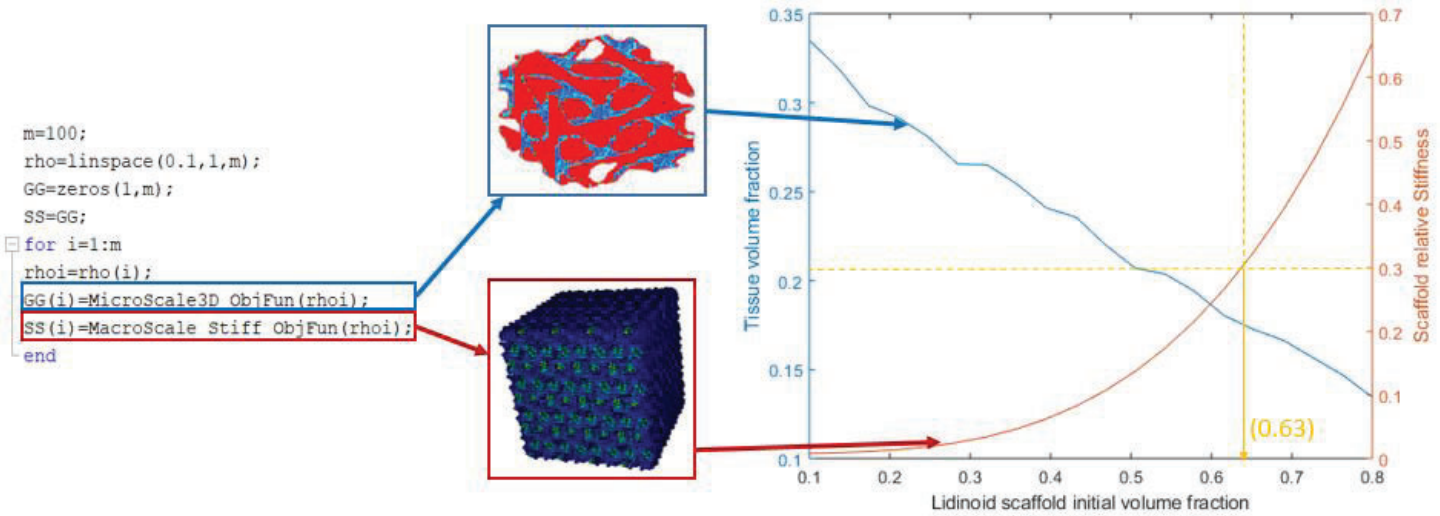

Figure 11: Visualization of how both the micro-scale tissue volume and the macro-scale scaffold stiffness vary with changing the scaffold volume fraction of the Lidinoid's cell type.

This multi-scale scheme provides an efficient way to determine the ideal geometry that leads to the maximum bone growth while still ensuring that the stiffness of the full-scale scaffold is high enough. Ideally the scheme should also take into account other physics fields involved in the bone generation process as well as Nano-scale

effects, these matters will be addressed in future work. Nevertheless, the scheme in its current state can already be used for an optimization.

Conclusion

A micro scale model to simulate the tissue generation in a cell seeded scaffold was successfully implemented and used to compare the volume of tissue generated after 40 days of culture with four different triply periodic minimal surface (TPMS) scaffolds. The Lidinoid cell type was found to have the best tissue generation capacity according to this curvature dependent model. The model has been validated with simpler geometries before by a different group but the validation was not considered thorough enough and this will be the subject of future work. The tissue generation model was also used to get an overview of how varying the volume fraction of a scaffold affects the volume developed after 40 days and it was found that the volume developed drops consistently as the volume fraction is increased.

The scaffold scale model to measure the mechanical performance was also implemented and initial results showed that the Lidinoid cell type has the highest stiffness. Moreover, using a numerical model developed based on a Finite Element Analysis, an overview of how the stiffness reacts to varying the volume density of the scaffolds was plotted. Lastly, regarding the multiscale optimisation, a suitable schematic has been set out, required parameters have been selected, a visual optimisation was carried out and suggestions were made for a suitable optimisation algorithm. The next steps of the project are to expand on the optimisation and then perform the experimental validation.

In the area of modelling the process of tissue regeneration in scaffolds, the ideal case in terms of accuracy is to have a model that involves all the physical processes that occur in vivo as well as all the length and time scales. However, in practice some of the physics fields or scales might not be as relevant for a given problem and would only add unnecessary complexity. For example, at this stage of the current project the interest is in finding optimal geometry parameters for a tissue generation scaffold; thus including the effect of fluid flow parameters or growth factors is not necessary. To conclude, although an existing challenge is to model all the different processes and scales involved in tissue generation scaffolds, the best scaffold would not necessarily be one that couples all the fields and scales but rather one that couples the required fields and scales to tackle a given problem most efficiently.

Future work

Regarding the modelling, there is still some work needed to improve the Finite Element Macro-scale model and the Multiscale optimization still needs to be carried out using MATLAB. Moreover, the experimental validation of the 3D tissue generation model and the scaffold's mechanical performance model still needs to be done. The effect of growth factors on the performance of tissue generation scaffolds will also be analyzed in the future in order to have a multi physics multiscale model.

References

[1] G. Zimmermann and A. Moghaddam, "Allograft bone matrix versus synthetic bone graft substitutes," *Injury*, vol. 42, pp. S16–S21, 2011.

[2] W. Wang and K. W. K. Yeung, "Bone grafts and biomaterials substitutes for bone defect repair: A review," *Bioact. Mater.*, vol. 2, no. 4, pp. 224–247, Dec. 2017.

[3] H. Ma, C. Feng, J. Chang, and C. Wu, "3D-printed bioceramic scaffolds: From bone tissue engineering to tumor therapy," *Acta Biomater.*, vol. 79, pp. 37–59, 2018.

[4] S. C. Kapfer, S. T. Hyde, K. Mecke, C. H. Arns, and G. E. Schröder-Turk, "Minimal surface scaffold designs for tissue engineering," *Biomaterials*, vol. 32, no. 29, pp. 6875–6882, 2011.

[5] S. Vijayavenkataraman, # Lei Zhang, S. Zhang, J. Ying, H. Fuh, and W. F. Lu, "Triply Periodic Minimal Surfaces Sheet Scaffolds for Tissue Engineering Applications: An Optimization Approach toward

Biomimetic Scaffold Design," 2018.
[6] E. Gamsjäger, C. M. Bidan, F. D. Fischer, P. Fratzl, and J. W. C. Dunlop, "Modelling the role of surface stress on the kinetics of tissue growth in confined geometries," *Acta Biomater.*, vol. 9, pp. 5531–5543, 2013.
[7] D. Eglin *et al.*, "Surface curvature in triply-periodic minimal surface architectures as a distinct design parameter in preparing advanced tissue engineering scaffolds," *Biofabrication*, vol. 9, no. 2, p. 025001, 2017.
[8] J. Manuel, G. Aznar, C. Valero, Carlos Borau, and N. Garijo, "Computational mechano-chemo-biology: a tool for the design of tissue scaffolds." 2012.
[9] C. M. Bidan, K. P. Kommareddy, M. Rumpler, P. Kollmannsberger, P. Fratzl, and J. W. C. Dunlop, "Geometry as a Factor for Tissue Growth: Towards Shape Optimization of Tissue Engineering Scaffolds," 2013.
[10] M. Rumpler, A. Woesz, J. W. C. Dunlop, J. T. Van Dongen, and P. Fratzl, "The effect of geometry on three-dimensional tissue growth." 2012.
[11] Y. Guyot *et al.*, "A computational model for cell/ECM growth on 3D surfaces using the level set method: a bone tissue engineering case study," *Biomech Model Mechanobiol*, vol. 13, pp. 1361–1371, 2014.
[12] J.A. Sethian, *Fast Marching Methods and Level Set Methods for Propagating Interfaces*. 1999.
[13] R. Huiskes and E. Y. S. Chao, "A SURVEY OF FINITE ELEMENT ANALYSIS IN ORTHOPEDIC BIOMECHANICS: THE FIRST DECADE," vol. 16, no. 6, pp. 385–409, 1983.
[14] I. Maskery, A. O. Aremu, L. Parry, R. D. Wildman, C. J. Tuck, and I. A. Ashcroft, "Effective design and simulation of surface-based lattice structures featuring volume fraction and cell type grading," *Mater. Des.*, vol. 155, pp. 220–232, Oct. 2018.
[15] N. A. Chartrain, C. B. Williams, and A. R. Whittington, "A review on fabricating tissue scaffolds using vat photopolymerization," *Acta Biomater.*, vol. 74, pp. 90–111, 2018.